FEASIBILITY OF MAINTAINING NATURAL CONVECTION MODE CORE COOLING IN RESEARCH REACTOR POWER UPGRADES

J. J. Ha, M. Belhadj, T. Aldemir, R. N. Christensen
The Ohio State University
Columbus, Ohio, U.S.A.

ABSTRACT

Two operational concerns for natural convection cooled research reactors using plate type fuels are: i) pool top ^{16}N activity (PTNA), and, ii) nucleate boiling in core channels. The feasibility assessment of a power upgrade while maintaining natural convection mode core cooling requires adressing these operational concerns. Previous studies have shown that:

- The conventional technique for reducing PTNA by plume dispersion may not be effective in a large power upgrade of research reactors with small pools.
- Currently used correlations to predict onset of nucleate boiling (ONB) in thin, rectangular core channels are not valid for low-velocity, upward flows such as encountered in natural convection cooling.

The PTNA depends on the velocity distribution in the reactor pool. COMMIX-1A code is used to determine the three-dimensional velocity fields in The Ohio State University Research Reactor (OSURR) pool as a function of varying design conditions, following a power upgrade to 500 kW with LEU fuel. It is shown that a sufficiently deep stagnant water layer can be created below the pool top by properly choosing the disperser flow rate. The ONB heat flux is experimentally determined for channel gaps and upward flow velocities in the range 2mm-4mm and 3-16 cm/sec., respectively. Two alternatives to plume dispersion for reducing PTNA and a new correlation to determine the ONB heat flux in thin, rectangular channels under low-velocity, upward flow conditions are proposed.

INTRODUCTION

Maintaining the core cooling mode in the power upgrade of natural convection cooled research reactors reduces the facility modifications and licensing issues to be addresed. Two operational concerns in the feasibility assessment of such an upgrade are: i) pool top ^{16}N activity (PTNA), and, ii) nucleate boiling in core channels.

The conventional technique for reducing PTNA is to disperse the active water plume rising above the core by a flat water jet. The PTNA depends on the pool velocity field under dispersion. Ideally, a sufficiently deep stagnant water layer is created below the pool top which confines ^{16}N activity to lower pool regions and also acts as a shield. Nucleate boiling in reactor channels leads to reactivity fluctuations which are operationally undesirable. Furthermore, onset of nucleate boiling (ONB) is usually regarded as a first warning to burnout in the safety assessment of plate type research reactors and is not allowed under normal operation.

Previous studies[1,2] have shown that:

- The conventional technique for reducing PTNA may not be effective in a large power upgrade of research reactors with small pools.

- Currently used correlations to predict the ONB heat flux in research reactors (i.e. Bergles-Rohsenow[3] and Ricque-Siboul[4] correlations) are not valid for low-velocity, upward flows in thin, rectangular channels such as encountered in natural convection cooled plate type research reactors.

The objectives of this study are:

1. Investigate the feasibility of using plume dispersion and two other alternatives for reducing PTNA in the power upgrade of natural convection cooled research reactors.

2. Experimentally determine the ONB heat flux in thin, rectangular channels as a function of upward flow velocity and channel gap, and find a new relation for correlating the ONB heat flux to flow parameters.

The system under consideration for objective #1 is The Ohio State University Research Reactor (OSURR) following a power upgrade to 500 kW with standardized[5] LEU fuel plates in a 16-plate (+2 dummy plates) standard and 10-plate control element geometry[6]. COMMIX-1A code[7] is used to simulate the three-dimensional pool dynamics under varying design conditions. The experimental setup for objective #2 and the present OSURR pool configuration, including the HEU core, are described in earlier work[1,2,6].

POOL DYNAMICS OF OSURR UNDER VARYING DESIGN CONDITIONS[8]

The OSURR core following the LEU conversion/upgrade is assumed to have 18 standard elements (i.e. core I in Ref.9). The options under consideration for reducing PTNA are schematically shown in Figs. 1-3. Option 1 uses the conventional technique for reducing PTNA. Options 2 and 3 are alternative techniques. The shroud in option 3 is an

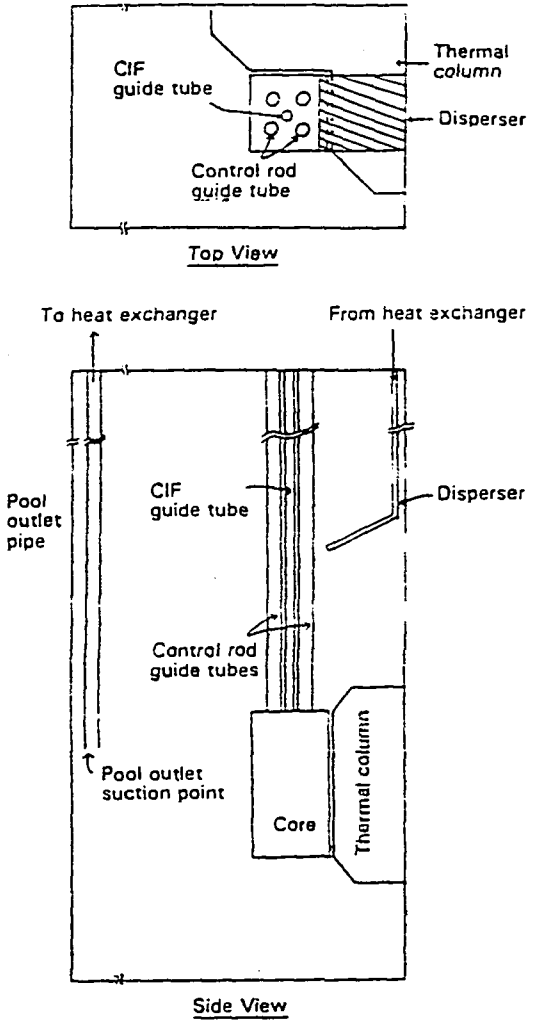

Fig. 1. OSURR pool configuration following conversion/ upgrade—option 1.

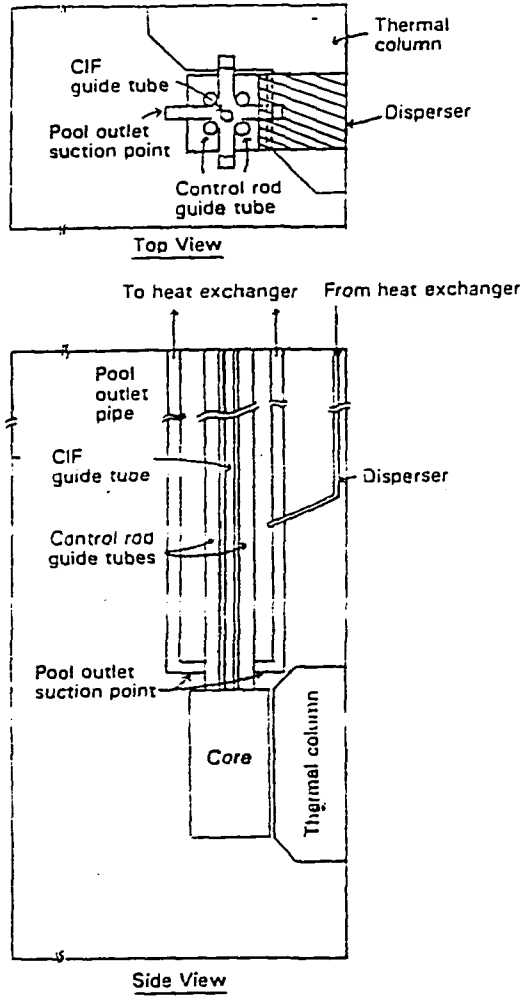

Fig. 2 OSURR pool configuration following conversion/ upgrade—option 2.

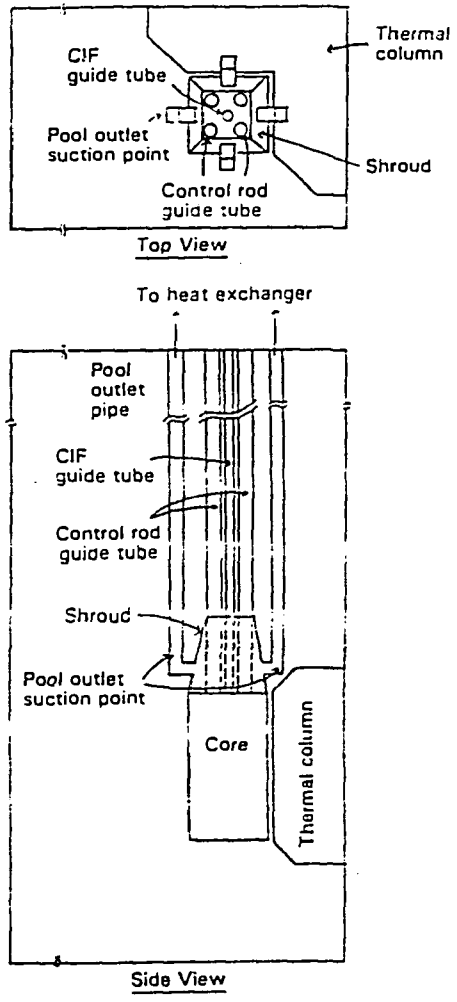

Fig.3. OSURR pool configuration following conversion/ upgrade—option 3.

aliminum box with a hole at the top to accomodate the guide tubes and to allow natural circulation if the heat removal system pump trips.

The computational model for COMMIX-1A simulations is similar to that described in Ref.1. However, two improvements are:

- The difference between the shapes of the guide tubes (circular) and the computational cells (rectangular) are accounted for using the concept of directional surface permeability[7]. In the previous study[1], the guide tubes are described as square ducts with equivalent cross-sectional area. This approximation leads to an exaggeration of jet flow diversion by the guide tubes and prediction of flow inversion in some core channels.

- In addition to laminar flow modeling with no frictional losses except in the core (physical model #1), turbulence effects are taken into consideration by: i) using generic correlations for cross-flow frictional losses in turbulent flow[7] at the guide tubes (physical model #2), or, b) assuming constant local turbulent viscosity and conductivity[7] (physical model #3).

Table I lists the characteristics of the cases considered in this study for options 1-3 shown in Figs. 1-3. Cases A-F, G and H-K correspond to options 1, 2 and 3, respectively. In all the cases the reactor power is 500 kW. Comparison of the results for cases A-F lead to the following observations:

TABLE I

Case Characteristics

Case	Disperser Inclination Angle (deg)	Shroud Height (m)	Disperser/Suction Velocity[a] (m/s)	Disperser/Suction Flow Rate[a] ($\times 10^{-2}$ m^3/s)	Physical Model Number
A	0	---	0.51	0.4935	1
B	30	---	0.51	0.4935	1
C	0	---	1.53	1.4805	1
D	30	---	1.02	0.6742[b]	1
E	30	---	0.51	0.4935	3
F	30	---	0.51	0.4935	2
G	0	---	1.00	0.9676	1
H	---	0.3620	0.17	0.3948	1
I	---	0.3620	0.22	0.5110	1
J	---	0.7811	0.17	0.3948	1
K	---	0.7811	0.22	0.5110	1

[a]For dispersers in cases A through G and at each suction point for cases H through K. The disperser location is 1.17 m above the core top (cases A through F). The location of the core outlet/suction points is far away from the core for cases A through F and 0.11 m above the core top for cases G through K. The pool heat removal system return water temperature is 20°C.
[b]Different disperser area.

1. Variation in disperser orientation (i.e. inclination angle in Table 1) has little effect on the pool velocity distribution.

2. The plume can be dispersed more effectively by increasing the

disperser mass flow rate.

3. A stagnant layer can be created below the pool top by the appropriate choice of the disperser mass flow rate. For the flow rates considered in cases C and D, the depth of the stagnant layer increases with increasing disperser mass flow rate (see Figs.4 and 5).

4. Physical model #1 underestimates the extent of plume dispersion and leads to conservative predictions with respect to PTNA, since cross-flow frictional losses (i.e physical model #2) improve plume dispersion. On the other hand, local turbulance effects (i.e. physical model #3) do not lead to significant changes in the predicted pool velocity distribution.

Assuming a uniformly distributed volume source under the stagnant layer, the OSURR pool top ^{16}N dose rate for case C is estimated to be <1mrem/h. However, as shown in Ref.1, observation #3 may not be valid if the reactor pool is small and high-velocity disperser flow is needed to overcome the plume momentum resulting from a large power increase. Interaction of the disperser jet with the opposite wall causes massive upward flow and prevents the stratification observed in Figs. 4 and 5. In that situation, an alternative to plume dispersion to reduce PTNA is to place the core outlet suction point near the top of the core (i.e option 2). Case G results show that the pressure drop due to the suction effect at the core outlet creates a deeper stagnant layer compared to cases C and D (see Figs.4, 5 and 6) and the disperser is redundant.

If the research reactor is undergoing a power increase that necessitates the upgrade of the existing heat exchanger or the installation of a new one (as is the case for OSURR), upgrade costs can be reduced by increasing the temperature difference between the primary and secondary sides of the heat exchanger and thus reducing the heat exchanger area needed for energy removal. Case A-G results show that the water temperature at the suction points is close to the average pool temperature ($\sim 25^{o}C$). Since the lower bound on the secondary side temperature is often determined by atmospheric conditions, the only way to accomplish cost reduction in the upgrade with options 1 and 2 is to increase the average pool temperature. On the other hand, increasing the average pool temperature may not be feasible, since: i) excessive evaporation from the pool may cause corrosion problems in the reactor hall, ii) reactor water cleanup system may degenerate, and, iii) increased core inlet temperature may lead to nucleate boiling in reactor channels.

Option 3 provides a way to increase heat exchanger primary side inlet temperature without increasing the average pool temperature. The results of case H show that, with the placement of the shroud above the core, the suction temperature rises by $13^{o}C$ (see Table II). Comparison of the results for cases I, J and K (see Table II and Fig. 7) indicates

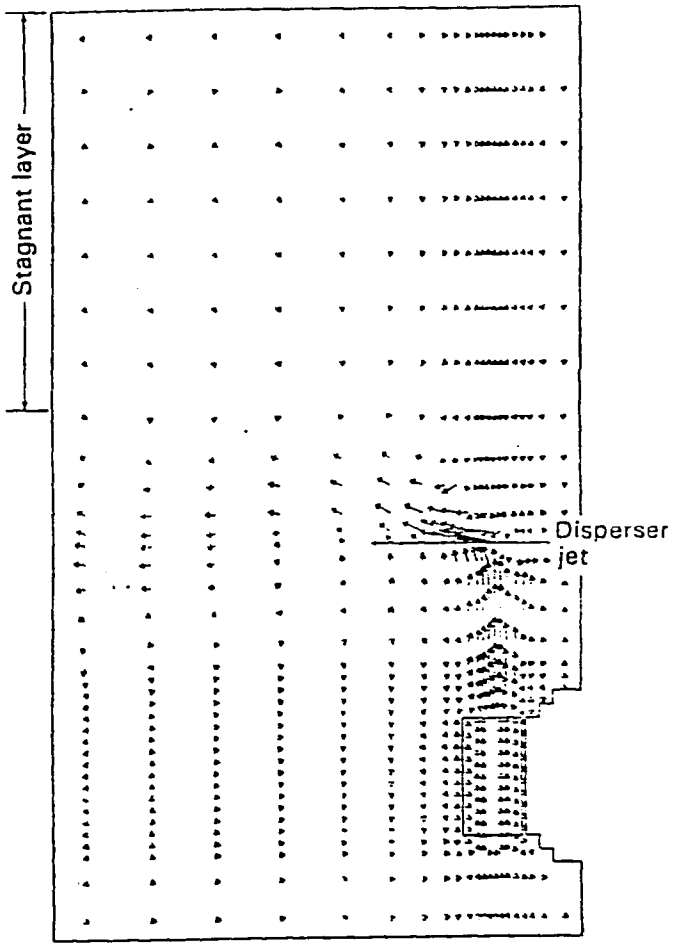

Fig. 4. OSURR pool velocity distribution—case C.

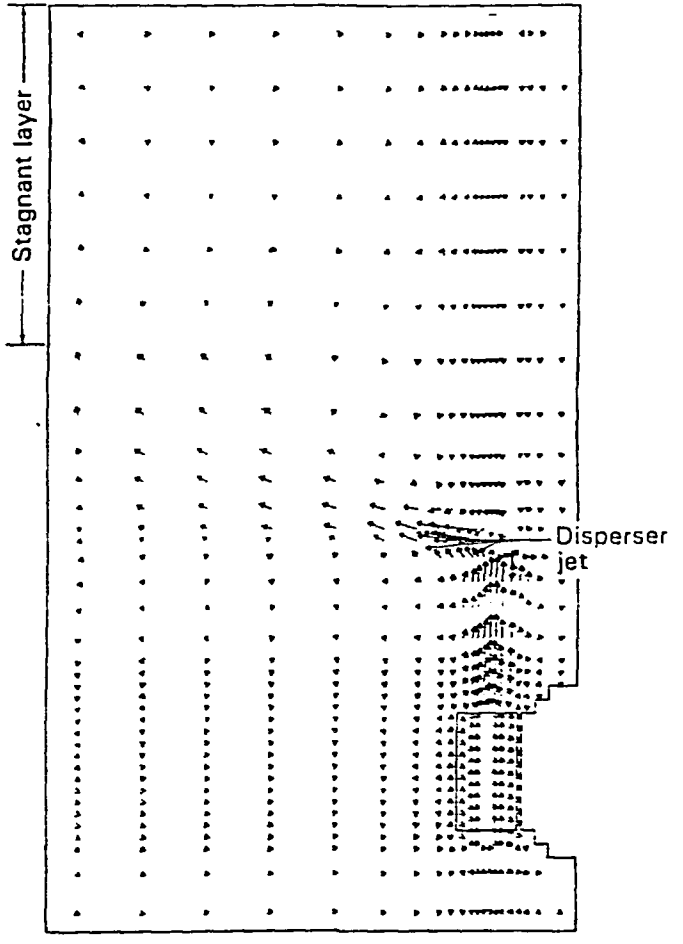

Fig. 5. OSURR pool velocity distribution—case D.

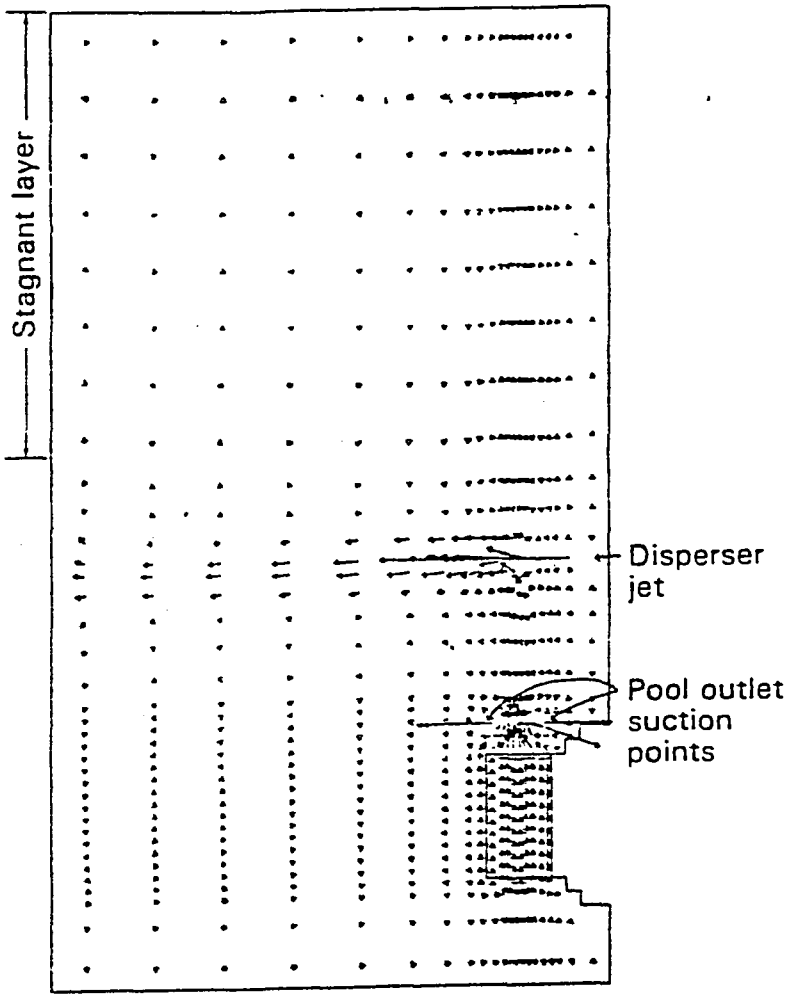

Fig.6 . OSURR pool velocity distribution—case G.

TABLE II

Comparison of Core Outlet Temperature, Suction Temperature, and Maximum Core Flow Velocity for Cases G Through K

Case	Maximum Standard Element (Control Element) Outlet Temperature (°C)	Suction Temperature (°C)	Maximum Core Flow Velocity (cm/s)
G	45.5(50.0)	28.7	11.3
H	51.0(52.1)	41.69	8.4
I	50.9(52.1)	41.15	8.2
J	45.5(49.3)	38.34	10.0
K	44.6(48.8)	37.90	10.2

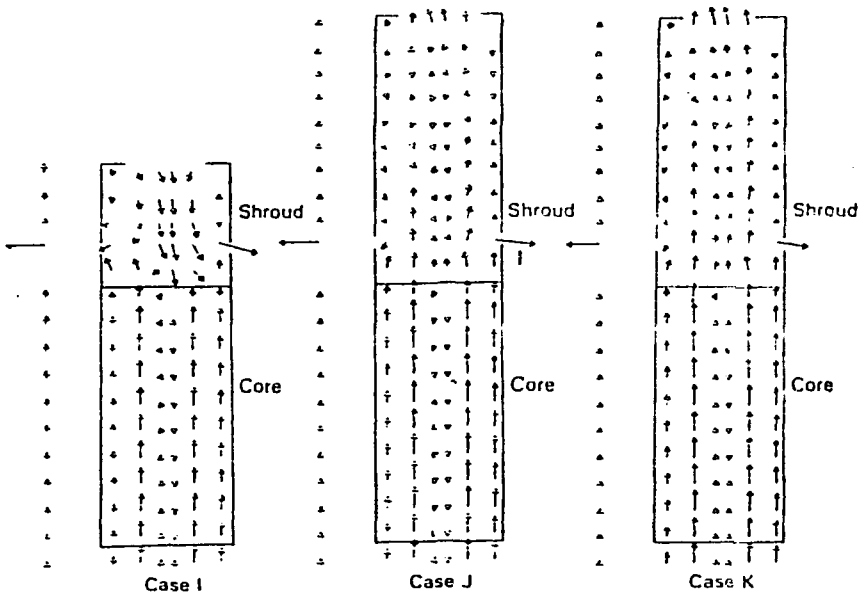

Fig. 7 . Velocity distribution within the shroud—cases I, J, and K.

the following:

- Due to high flow resistance of the core, channel flow velocities and core outlet temperature are not appreciably affected by an increase in the suction rate. However, since the flow resistance of the hole on top of the shroud is very small, the resulting pressure drop increases cool water inflow into the shroud and subsequently decreases the suction temperature.

- The chimney effect becomes prominent with increasing shroud height. Some portion of the plume escapes the shroud due to increased channel velocities. Water temperature at the suction point again decreases.

Thus to maximize the heat removal system primary inlet temperature and minimize PTNA, the shroud should not extend beyond the top hole on the control guide tubes.

ONSET OF BOILING IN THIN RECTANGULAR CHANNELS UNDER LOW-VELOCITY UPWARD FLOW

Experimental Procedure

The experimental setup is described in Ref. 2. The control parameters are the channel gap, average flow velocity and heat flux. Heat source distribution along the channel wall has a truncated cosine shape to simulate the axial neutron flux distribution in the fuel plate (and the hence energy production rate). A total of 18 experiments were carried out to determine the ONB heat flux as a function of the local flow parameters. Table III shows the case characteristics for each experiment. The static pressure head at the channel exit (1.5 atm. absolute) and channel wall surface roughness are assumed to be constant for all the cases. For the visual determination of ONB, the ONB point is defined as the first location on the channel surface at which bubbles start to form.

For data reduction, the definition of Reynolds number based on channel thickness is used[10], i.e.,

$$Re=\rho\, vd/\mu = \dot{m}/\mu\, w. \qquad (1)$$

Here ρ and μ are local water density and local viscosity, respectively. The parameters v, d, $\dot{m}$, and w=6.7cm. indicate the channel velocity, gap size, mass flow rate and constant channel width, respectively. In the determination of the Reynolds number, $\dot{m}$ is measured. Local viscosity is found from property tables by:

- linear interpolation of the measured channel inlet and outlet pressures to estimate the local pressure, and,

estimating the local enthalpy, $h_l(z)$, from

$$h_l(z)=h_i+(w/\dot{m}) \int_0^z q''(z')\, dz'. \qquad (2)$$

In Eq.(2), h_i is the channel inlet enthalpy (known from measured pressure and temperature) and q"(z) is the surface heat flux distribution (measured at 11 points along the channel). The integration is performed using one-third Simpson's rule[11].

TABLE III

Case Characteristics for CNB Experiments

Case	Average Channel Velocity (cm/s)	Channel Gap (mm)	Case	Average Channel Velocity (cm/s)	Channel Gap (mm)
1	4.0	3.0	10	6.0	4.0
2	5.0	3.0	11	7.0	4.0
3	7.0	3.0	12	6.0	2.0
4	8.0	3.0	13	8.0	2.0
5	10.0	3.0	14	10.0	2.0
6	12.0	3.0	15	12.0	2.0
7	3.0	4.0	16	14.0	2.0
8	4.0	4.0	17	16.0	2.0
9	5.0	4.0	18	8.0	4.0

Observations

For low heat fluxes, the energy transfer mechanism into the channel is forced convection. Bubbles start forming on the surface with increasing heat flux (Fig. 8.a). However, the bubble growth may not be stable and bubbles often collapse at the same location. Figs.8.a and 8.b illustrate the reduction in bubble size within 10 sec. for case #8. Initiation of bubble formation marks the beginning of the transition regime into nucleate boiling. As the heat flux further increases, the bubbles start to leave the surface (Fig. 8.c) or slide upward along the channel surface (Fig. 8.d), and nucleate boiling begins. Note that this definition of nucleate boiling is different from its conventional definition which only considers bubble departure from the surface and not bubble motion along the channel wall. As will be shown later, bubble motion along the channel wall can also remove the energy deposited in the bubble vapor out of the channel and in this respect is included in the definition of nucleate boiling. Eventually, nucleate boiling develops into fully developed boiling, which is characterized by severe bubble agitation (Fig. 8.e), and leads to pressure oscillations in the channel.

a (Case #8) b (Case #8) c (Case #3) d (Case #12) e (Case #13)

Fig. 8 Bubble formation and nucleate boiling in thin, rectangular channels

For Re<450, it was observed that bubbles can grow very large on the surface and may cause a reduction in channel flow area (Figs. 8.c, 8.d). These bubbles are then pushed upward along the surface by the flow until they either: i) reach a colder surface and collapse, or, ii) reach a hotter surface and depart into the flow. Bubble growth and subsequent reduction in the flow area does not disturb the laminar nature of the flow. Two bubbles growing on the opposite channel walls sometimes join (Figs. 9.a and 9.b) and sweep all the bubbles on the two surfaces as they move upward, forming a vapor column. In that case, the energy deposited in the bubbles is removed out of the channel in the form of a vapor slug.

For 450<Re<700, the transition regime into nucleate boiling is characterized by stable bubble growth on the channel surface (Fig.9.c). Comparison of Figs.8.a or 8.b with Fig.9.c shows that the bubble size is decreased for higher Reynolds numbers at the transition regime. On the other hand, bubble growth frequency on the channel surface increases both for the transition and nucleate boiling regimes. There is little upward bubble motion along the channel wall and the bubbles continuously grow and depart from the surface (Figs.9.d and 9.e), with less chance for flow area restriction even for a 2mm. channel gap.

For Re>700, some turbulence was observed in the transition region to nucleate boiling. The magnitude of the turbulence increases with increasing Reynolds number. The frequency of bubble formation on the channel surfaces also increases, with decreasing bubble size before departure into the flow. For case #18, turbulence occured even in the forced convection regime, with accompanying pressure oscillations in the channel and wall temperature oscillations of almost 3^{0}C. Thus no valid data could be obtained for case #18.

Results and Analysis

Table IV lists the ONB heat fluxes ($q"_{ONB}$) and wall superheats (ΔT_{sat}) for each case, as well as the corresponding Reynolds numbers. In Fig. 10, the experimental data are shown graphically and compared to the predictions by the correlations conventionally used to predict $q"_{ONB}$ in research reactor channels. From Fig.10 it is clear that: a) there is no general trend relating $q"_{ONB}$ to ΔT_{sat}, and, b) the Bergles-Rohsenow and Ricque-Siboul correlations over- and underestimate $q"_{ONB}$, respectively. For Re>650, most of the experimental data are predicted well by the Bergles-Rohsenow correlation. This agreement is not surprising since the Bergles-Rohsenow correlation is derived and validated for turbulent flow.

The graphical description of the $q"_{ONB}$ data in Table IV (see Fig.11) against Re implies a correlation of the form:

$$q"_{ONB}=aRe^{b+c/d} \qquad (3)$$

Here a, b and c are fitting parameters. Least-squares fitting of

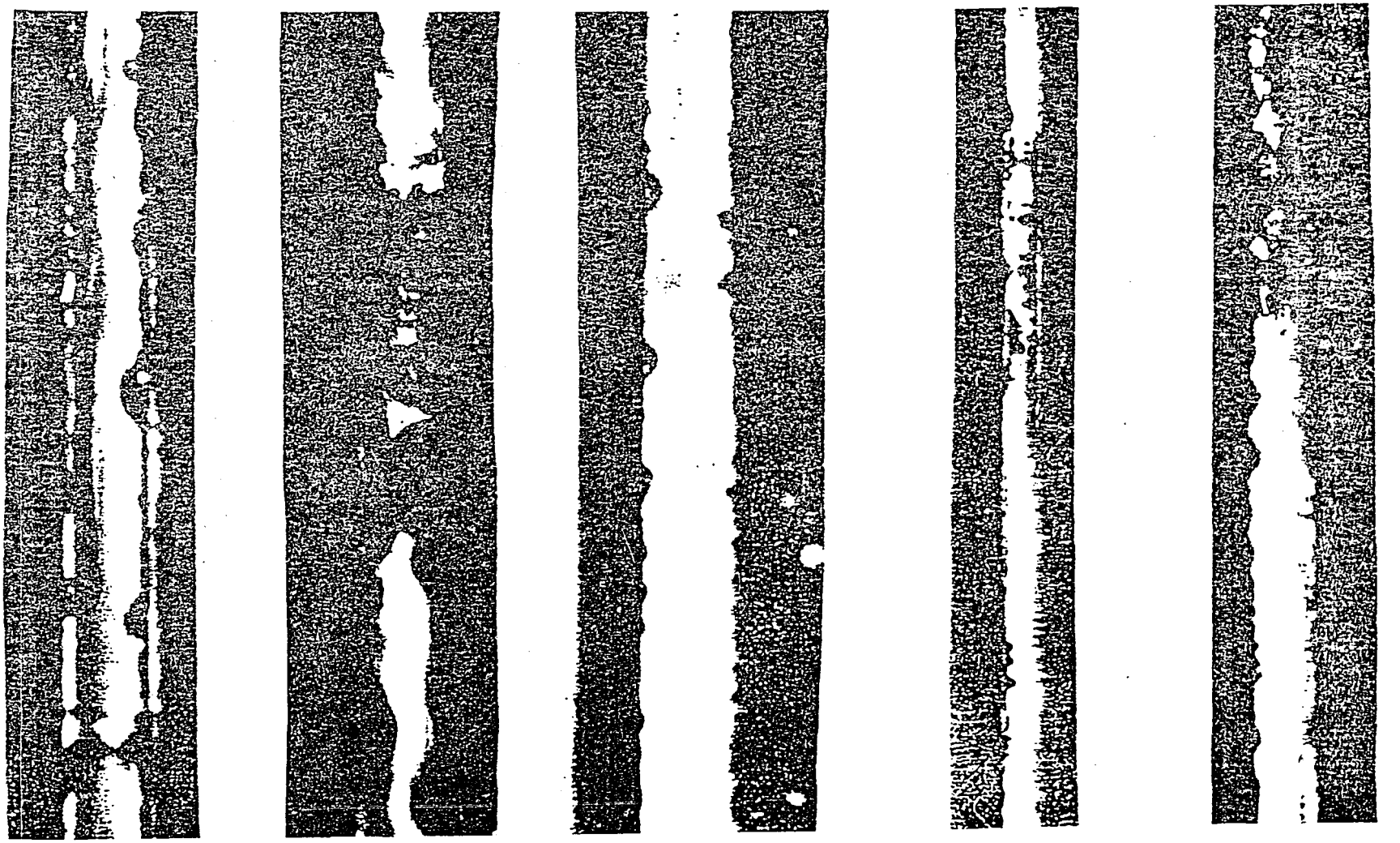

a (Case #13) b (Case #12) c (Case #10) d (Case #3) e (Case #10)

Fig. 9 Bubble formation and nucleate boiling in thin, rectangular channels

TABLE IV

Summary of Experimental Results

Case	q''_{ONB} (KW/m^2)	ΔT_{sat} (^oC) $\pm$ 0.3 ^oC	Re $\pm$ 6 %
1	15.1 $\pm$ 5.3	2.9	297
2	22.0 $\pm$ 5.3	3.0	382
3	33.2 $\pm$ 5.4	3.5	513
4	36.3 $\pm$ 5.5	2.8	539
5	43.9 $\pm$ 5.5	2.9	743
6	47.1 $\pm$ 5.6	3.0	922
7	16.6 $\pm$ 5.3	3.8	331
8	25.3 $\pm$ 5.4	3.5	479
9	31.3 $\pm$ 5.4	3.9	550
10	32.4 $\pm$ 5.4	3.1	656
11	33.6 $\pm$ 5.5	2.3	802
12	24.3 $\pm$ 5.3	2.4	343
13	35.2 $\pm$ 5.5	2.9	428
14	46.2 $\pm$ 5.6	2.9	548
15	59.9 $\pm$ 5.8	3.0	633
16	62.9 $\pm$ 5.8	3.1	680
17	66.2 $\pm$ 5.9	3.1	693

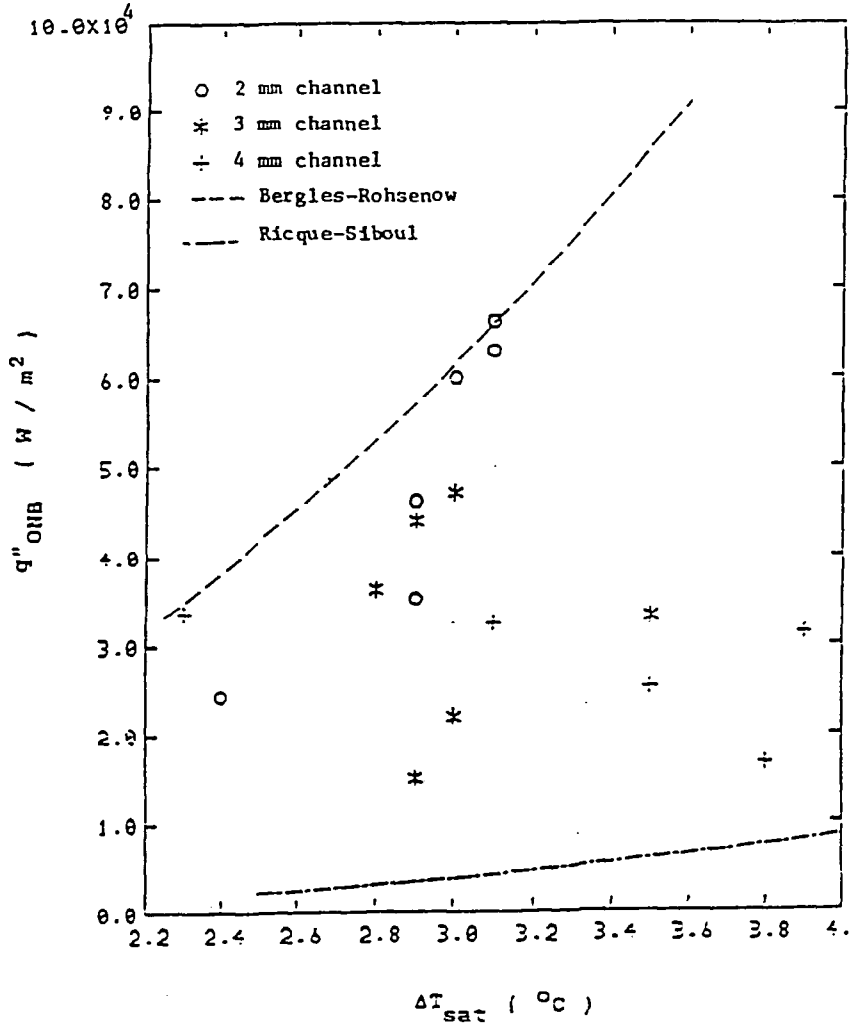

Fig. 10 Comparison of experimental results to predictions by the conventional correlations

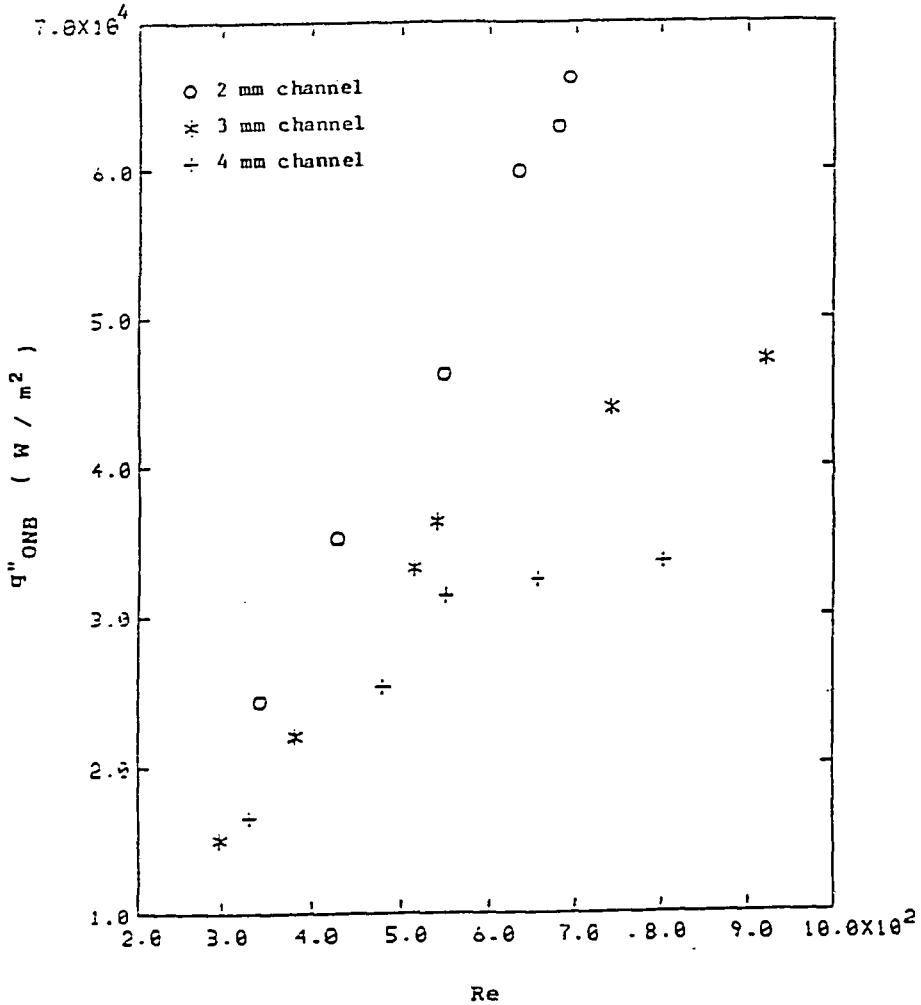

Fig. 11 Graphical description of the q''_{ONB} data in terms of Reynolds number

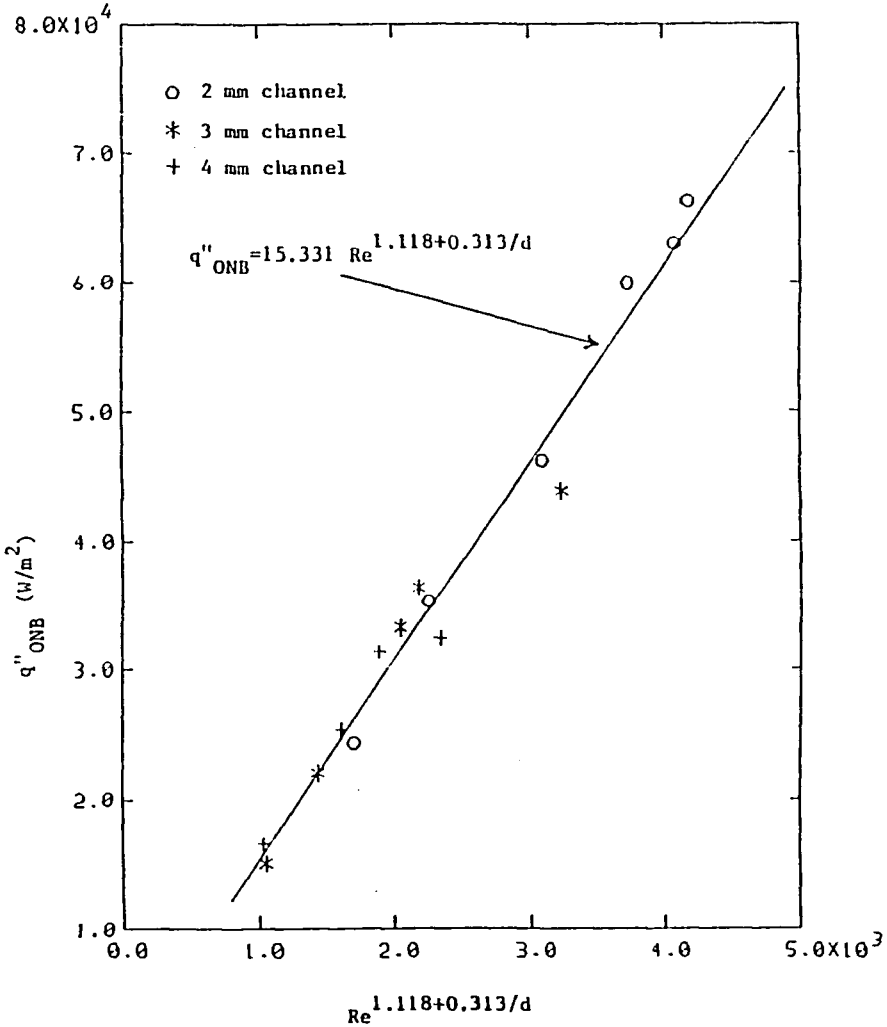

Fig. 12 Comparison of the experimental results to predictions by Eq.(3)

Eq.(3) to the data in Table IV for Re<750 yields a=15.331 W/m^2, b=1.118 and c=0.313 mm. The q''_{ONB} and d are in W/m^2 and mm., respectively. Fig.12 shows that Eq.(3) predicts the experimental data very well. The maximum discrepency between the predictions by Eq.(3) for Re<750 and Table IV results is less than 13% (case #5). Since the experimental error in determining q''_{ONB} and Re for case #5 are 13% and 6%, respectively (see Table IV), this discrepency is within the experimental error margin.

CONCLUSIONS

The results of the study show that:

1. The effectiveness of plume dispersion to reduce PTNA depends on the reactor power and pool dimensions. For reactors with small pools undergoing a large power increase, options #2 and #3 (see Figs. 2 and 3) may be more feasible. Option #3 also allows reducing the power upgrade costs.

2. For thin, rectangular channels under low-velocity, upward flow conditions, ONB heat flux is correlated to the local Reynolds number and channel gap size, and not the wall superheat. Under these conditions, the predictions by the Bergles-Rohsenow and Ricque-Siboul correlations constitute the upper and lower bounds on the ONB heat flux, respectively.

The results of the study also show that the LEU conversion/upgrade of OSURR to 500 kW is feasible with option #3, using a shroud height of 75-80 cms.(i.e. case J in Table I). This shroud height is not optimal with regard to upgrade costs, but allows maintaining an ONB ratio of 1.18-1.22, depending on the LEU core configuration used for the upgrade[9]. Case I in Table I (i.e. 36 cm. shroud height) maximizes the heat exchanger primary side inlet temperature, however, the data in Ref.9 and Tables II-IV indicate that ONB may occur in the core channels under the flow conditions corresponding to case I.

It is important to note that if option #3 is used to reduce PTNA, the core outlet pipe (see Fig. 3) has to be shielded, as well as thermally insulated. The water flowing through the pipe is active and may lead to high pool top doses if not shielded. Thermal insulation is necessary to prevent the heat losses through the pipe into the pool. In addition, a delay tank will be required to de-activate the inlet water to the primary side of the heat exchanger. In the conversion/upgrade of OSURR, the delay tank will be placed at the pool bottom. However, these additions to the existing facility are not expected to be as costly as installing a conventional downward-flow, forced-convection cooling system to accomplish the upgrade.

ACKNOWLEDGMENT

This study was partly supported by the U. S. Department of Energy Grant No. DE-FG02-85ER75201.A000.

REFERENCES

1. J. J. Ha, T. Aldemir, "Thermal-Hydraulic Analysis of the OSURR Pool for Power Upgrade with Natural Convection Core Cooling", to be published in the Proceedings of the 1986 International RERTR Meeting, ANL/RERTR/TM-9, Argonne National Laboratory.

2. M. Belhadj, R. N. Christensen, T. Aldemir, "Experimental Investigation of Onset of Nucleate Boiling in Thin Rectangular Channels", to be published in the Proceedings of the 1986 International RERTR Meeting, ANL/RERTR/TM-9, Argonne National Laboratory.

3. A. E. Bergles, W. M. Rohsenow, "The Determination of Forced-Convection Surface Boiling Heat Transfer", Journal of Heat Transfer, Trans. ASME, Series C, Vol.86,pp 365-371 (1964).

4. R. Ricque, R. Siboul, "Ebullition Locale de l'Eau en Convection Forcee", CEA R-3894, May 1970.

5. H. H. Young, J. E. Matos, "Conversion and Standardization of University Reactor Fuels Using Low-Enrichment Uranium-Plans and Schedules", to be published in the Proceedings of the 1986 International RERTR Meeting, ANL/RERTR/TM-9, Argonne National Laboratory.

6. M. D. Seshadri, T. Aldemir, "Neutronic Scoping Calculations for OSURR Core with Standardized U_3Si_2 Fuel Plates", to be published in the Proceedings of the 1986 International RERTR Meeting, ANL/RERTR/TM-9, Argonne National Laboratory.

7. H. M. Domanus, R. C. Schmitt, W. T. Sha, V. L. Shah, "COMMIX-1A: A Three Dimensional Transient Single-Phase Computer Program for Thermal-Hydraulic Analysis of Single and Multicomponent Systems, Volume I: Users' Manual", NUREG/CR-2896 Vol.1 (1983).

8. J. J. Ha, T. Aldemir, "Pool Dynamics of Natural-Convection-Cooled Research Reactors", to be published in the December 1987 issue of Nuclear Technology.

9. M. D. Seshadri, H. S. Aybar, T. Aldemir, "Neutronic Design of An LEU Core for The Ohio State University Research Reactor", these proceedings.

10. R. B. Bird, W. E. Stewart, E. N. Lightfoot," Transport Phenomena, John Wiley & Sons (1960).

11. M. C. Potter, Mathematical Methods in the Physical Sciences, Prentice-Hall (1978).